Applied Mathematics & Information Sciences
An International Journal

Two Pulse Designs for Ultra Wideband-Cognitive Radio by Using Multiple Modified Transform Domain Communication System

Shubin Wang[1],*Zheng Zhou*[2] *and Kyungsup Kwak*[3]

[1] College of Electronic Information Engineering, Inner Mongolia University, Hohhot 010021, China
[2] Wireless Network Lab., Beijing University of Posts and Telecommunications, Beijing 100876, China
[3] UWB Wireless Communications Research Center, Inha University, Incheon 402-751, Korea

Received: Jul 18, 2011; Revised Dec. 10, 2011; Accepted Jan. 26, 2012
Published online: 1 September 2012

Abstract: In order to adapt to all kinds of spectral mask and utilize the full frequency band and avoid interference to/from the existing wireless systems for ultra wideband (UWB), this paper investigates two pulse designs for ultra wideband-cognitive radio (UWB-CR) by using multiple modified transform domain communication system (M-TDCS). By applying multiple M-TDCS and installing a different power scale factor to each sub-band with about 1-2GHz, the first flexible and implementable pulse is generated. By using a combination of the multiple M-TDCS and compressed chirp waveform, the second pulse is accomplished. The two new pulses each can be implemented by surface acoustic wave (SAW) devices and some other accessorial devices as well, moreover, comparing with the seventh order derivative of Gaussian pulse, the bit error ratio (BER) performance by using these two pulses can be observably improved 2-3dB for UWB systems. For BER performance, the second pulse is better, but it is more complex.

Keywords: Pulse design, Ultra wideband-cognitive radio, M-TDCS, Compressed chirp.

1. Introduction

Recently, ultra wideband (UWB) [1] integrated with cognitive radio (CR) [2] (UWB-CR) has gained significant interest due to its ability to exploit the advantages and unique features of these two spectrum sharing techniques [3]. UWB can share the spectrum with some existing narrowband wireless systems, and CR can recognize the radio scene and regulate its communication scheme so as to utilize the frequency spectrum more efficiently and flexibly. While UWB-CR not only can utilize CR to implement collaborative coexistence schemes, but also can use UWB as a versatile PHY layer and adapt to various wireless channel conditions based on its inherent capability and scalability.

With dynamic spectrum allocation as a major task of CR, one of its functions is to select a modulation scheme which is used to adapt to the varying radio environment by utilizing spectrum holes. For the modulation strategy of CR, a natural choice of former study is the orthogonal frequency-division multiplexing (OFDM) by virtue of its flexibility and computational efficiency[4], and another suggestion is the transform domain communication system (TDCS) as a potential candidate as well [5]. The literature [6] gives a detailed description about the TDCS transmitter and its receiver system, and highlights the fundamental differences related to OFDM and multicarrier code-division multiple access (MC-CDMA).

With respect to UWB, two standards have been proposed, named as multi-band orthogonal frequency division multiplexing UWB (MB-OFDM-UWB) and direct-sequence UWB (DS-UWB) respectively [7,8]. In order to avoid interference to/from the existing wireless systems, MB-OFDM-UWB divides the UWB spectrum into many sub-bands, and meanwhile, deactivates some of sub-bands around these existing wireless systems (e.g. 5.3Hz in IEEE 802.11a WLAN frequency band); however, DS-UWB, being an impulse radio (IR) UWB, commonly generates a spectral notch to solve the interference problem [9]. UWB-CR, based on IR, can theoretically generate an adaptive

* Corresponding author: e-mail: wangsb09@gmail.com

UWB pulse waveform for avoiding interference. Depended on the linear combination of orthogonal prolate spheroidal wave functions (PSWF), the literature [3] investigates a design method of pulse waveform optimization, but PSWF needs a large quantity of calculation, so this waveform is only used in theoretical analysis, and is very difficult to implement for device.

Since US Federal Communication Commission (FCC) released a spectral mask with some restrictions [1] for ultra wideband in 2002, the research on UWB has been mainly centered on 3.1-10.6GHz frequency band based on FCC's UWB spectrum mask, however, the UWB mask is dissimilar in different countries or regions [1, 10], and so the variations of UWB mask should be taken into consideration and other frequency bands besides 3.1-10.6GHz should also be utilized.

The pulse compression technique of linear frequency modulated (FM) chirp waveform possesses high processing gain, and is widely used in radar systems [11]. The chirp waveform and its correlation process are easily accomplished by using surface acoustic wave (SAW) chirped delay lines [11, 12]. Based on the instantaneous frequency of the linear chirp waveform varying linearly with time, the literature [13] constructs a time-frequency mapping processing to modify chirp waveform. This scheme requires only time domain processing compared with TDCS, but this processing needs to accurately sense this extremely wide spectrum in real time because the UWB bandwidth is extra wide. However, any details about how to detect this extra wide spectrum are not mentioned in literature [13]. Moreover, the performance of the proposed scheme isn't superior to that of TDCS.

In this paper, we propose two pulses for UWB-CR based on multiple modified TDCS (M-TDCS). Both of two pulses use multiple M-TDCS to detect the UWB spectrum in real time, and can avoid interference to/from the existing wireless systems, and besides, the two pulses can use the full frequency band for any UWB spectrum masks, and can be implemented by SAW devices and some other accessorial devices as well.

The rest of this paper is organized as follows. Section 2 introduces simply the work procedure of TDCS and the basic theory of chirp waveform, and the proposal pulses for UWB-CR by using multiple M-TDCS are described in Section 3. Section 4 gives the simulation analysis, and the conclusions are drawn in Section 5.

2. A brief review for TDCS and chirp waveform

2.1. The work procedure of TDCS

With the assumption that both the transmitter and receiver are observing the same electromagnetic environment, the TDCS produces a complex sequence which avoids existing users or interferences by operating dynamically over a given bandwidth . A block diagram for the TDCS transmitter is shown in Figure 1. The TDCS transmitter firstly samples the radio environment, and then, the sampled values are compared with a hard limiting threshold to generate a vector $A'(w)$ representing an interference free spectrum of the radio environment. Amplitudes of $A'(w)$ exceeding the threshold are set as zero and the remainders are assigned to a value of one. Next, $A'(w)$ is multiplied by a multi-valued complex pseudorandom phase vector $e^{j\theta(w)}$ to get a new vector $B_b(w)$. In order to ensure that the communication symbols have the desired signal energies, $B_b(w)$ is subsequently amplitude-scaled by constant factor C. Finally the resultant spectral vector $B(w)$ takes the appropriate inverse Fourier transform to produce a time domain basis function (BF)$b(t)$, which can be stored and modulated in accordance with a data $d(t)$[5, 6].

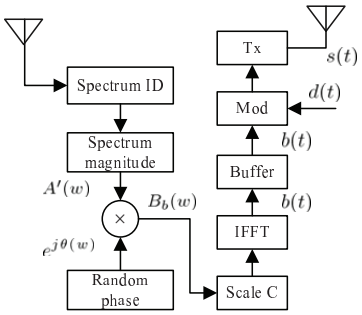

Figure 1 TDCS Transmitter.

2.2. The basic theory of chirp waveform

A chirp waveform [11, 14] may be expressed by

$$ch(t) = \begin{cases} \mathrm{g(t)}\cos(2\pi(f_0 t + \frac{\mu}{2}t^2) + \varphi_0), & |t| \le \frac{T_m}{2} \\ 0, & |t| > \frac{T_m}{2} \end{cases} \quad (1)$$

where $g(t)$,f_0,T_m are the chirp envelope, the center frequency, the chirp duration, respectively. φ_0 is the initial phase of the chirp waveform, and μ is the chirp rate (also named frequency sweep rate) and may be positive or negative. When $\mu > 0$, $ch(t)$ is called an up-chirp,when $\mu < 0$, $ch(t)$ is called a down-chirp.

The instantaneous frequency of chirp waveform can be written as

$$f_{ch}(t) = \frac{1}{2\pi}\frac{d(2\pi(f_0 t + \frac{\mu}{2}t^2) + \varphi_0)}{dt} = f_0 + ut \quad (2)$$

From (2),the $f_{ch}(t)$ and t maintain a linear relationship, and the chirp rate μ remains constant in each chirp duration. The bandwidth B_s of $ch(t)$ is corresponding to frequency-sweep range which can be defined as $B_s = |\mu| *$

T_m . When frequency-sweep is stopped, the instantaneous bandwidth of $ch(t)$ depends on $g(t)$. Typical choices of $g(t)$ include [14]: (1) a rectangular window with amplitude 1 and duration T_m centered at $t = 0$ as follows $g(t) = \prod(t/T_m)$, and (2) a truncated Gaussian pulse shown as follows $g(t) = \prod(t/T_m)(\frac{1}{\sqrt{2\pi\sigma}}e^{-\frac{t^2}{2\sigma^2}})$.

When $g(t) = \prod(t/T_m)$, the autocorrelation function of $ch(t)$ is given as [12, 14]

$$p_c(t) = \sqrt{B_s T_m}\frac{\sin(\pi B_s t(1-\frac{|t|}{T_m}))}{\pi B_s t}\cos(2\pi f_0 t), |t| \le T_m \quad (3)$$

Because the energy of $p_c(t)$ is concentrated in the center of time compared with $ch(t)$, $p_c(t)$ is also named compressed chirp waveform.

3. Proposal pulses for UWB-CR

In this section, we describe the two proposal pulses for UWB-CR by using multiple M-TDCS.

3.1. The M-TDCS and first proposal pulse

3.1.1. M-TDCS

The TDCS can dynamically sense the radio environment and generate a time domain BF, so we only modify appropriately the time domain BF to meet the requirement of UWB mask, and the first UWB-CR pulse can be obtained.

The phase vector $e^{j\theta(w)}$ of TDCS mainly ensures that the time domain BF has correlation properties similar to that of a noise signal in military application, but it is better that the energy of a UWB pulse is concentrated on the center of the time, so we abridge the vector $e^{j\theta(w)}$. There are different UWB masks for the different countries or regions, we use a "UWB Spectrum Masks" module to provide different UWB masks–$Mask_j(f)$. Because the UWB frequency spectrum is extremely wide, in order to sense rapidly the radio environment to satisfy the requirement of UWB-CR on the dynamic spectrum allocation and the power control, we divide the UWB frequency band into M continuous sub-bands $B_m(m = 1, 2, ...M)$, accordingly, we give a mask value $Mask_{jm}(f)$ for each sub-band based on $Mask_j(f)$. Finally, the power scale factor C of TDCS is replaced by the mask value $Mask_{jm}(f)$, so the M-TDCS is obtained.

The TDCS is actually a digital communications architecture, so we express BF with $b(n)$ instead of $b(t)$. Let each sub-band B_m employ one M-TDCS to generate one sub-BF $b'_m(n)$, and sum M sub-BFs to get a new time domain BF $b'(n)$. After the signal $b'(n)$ is converted by DAC device, a new pulse named $S_{UWB-CR1}(t)$ for UWB-CR can be obtained. A block diagram of M-TDCS is illustrated in Figure 2, and first proposal pulse is illustrated in Figure 3.

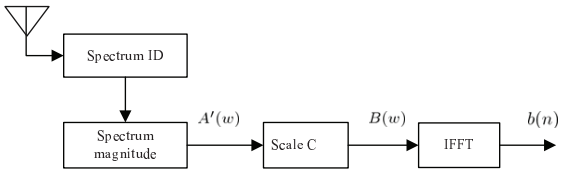

Figure 2 M-TDCS scaled by the mask value $Mask_{jm}$.

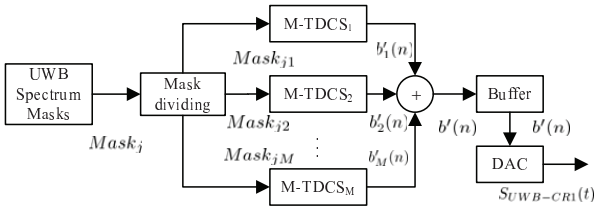

Figure 3 The first pulse design for UWB-CR by using multiple M-TDCS .

Depended on the above work, $b'(n)$ can be expressed as

$$\begin{aligned} b'(n) &= \sum_{m=1}^{M} b'_m(n) \qquad n = 1, 2, ..., N \\ &= \sum_{m=1}^{M}\frac{1}{N}\sum_{l=1}^{N} A'_m Mask_{jm} e^{-j(2\pi(l-1)(n-1)/N)} \end{aligned} \quad (4)$$

where N is the point number of inverse Fourier transform.

3.1.2. Generating the mask value

In (4), the values of the vector A'_m are "1" or "0", so the crucial task of $b'(n)$ is to gain $Mask_{jm}(f)$ depending on the selected mask $Mask_j(f)$.

For IR-UWB, two signal schemes are adopted, named DS-UWB and time-hopping (TH) UWB. The commonly adopted modulation schemes of these two signals include pulse position modulation (PPM) and pulse amplitude modulation (PAM) [15–20].

PPM-TH-UWB, PAM-TH-UWB can be expressed by (5), (6), respectively.

$$S_1^{(k)}(t) = \sqrt{\frac{\varepsilon_s}{N_s}}\sum_{j=-\infty}^{\infty} p(t - jT_s - C_j{}^{(k)}T_d - \varepsilon d^{(k)}_{\lfloor j/N_s \rfloor}) \quad (5)$$

$$S_2^{(k)}(t) = \sqrt{\frac{\varepsilon_s}{N_s}}\sum_{j=-\infty}^{\infty} e^{(k)}_{\lfloor j/N_s \rfloor} p(t - jT_s - C_j{}^{(k)}T_d) \quad (6)$$

In (5), (6), K , T_s , ε_s denote the index of user and the pulse repetition time and the symbol energy, respectively. $C_j{}^k$ is a TH sequence (also named pseudorandom (PN) code) of the k^{th} user, and the period of TH sequence is N_p .T_d is a delay time governed by TH sequence, and ε

is a constant. As shown in $d^{(k)}_{\lfloor j/N_s \rfloor} \in \{0,1\}$, $e^{(k)}_{\lfloor j/N_s \rfloor} \in \{-1,+1\}$, $\lfloor\ \rfloor$ represents an integer operator. $p(t)$ is the pulse waveform with a duration time T_b , $T_b \ll T_s$. For a fixed T_s , the symbol rate R_s determines the number N_s of $p(t)$ which is modulated by a given binary symbol via $R_s = 1/(N_s T_s)$.

PPM-DS-UWB, PAM-DS-UWB can be expressed by (7), (8), respectively.

$$S_3^{(k)}(t) = \sqrt{\frac{\varepsilon_s}{N_s}} \sum_{j=-\infty}^{\infty} \sum_{n=1}^{N_r} a_n^{(k)} p(t - jT_r - nT_c - \varepsilon b_j^{(k)}) \quad (7)$$

$$S_4^{(k)}(t) = \sqrt{\frac{\varepsilon_s}{N_s}} \sum_{j=-\infty}^{\infty} \sum_{n=1}^{N_r} a_n^{(k)} b_j^{(k)} p(t - jT_r - nT_c) \quad (8)$$

In (7) and (8), ε_s , k are the same as in (5) and (6). T_r is the duration for each data bit, and j is the index for the data bit. The data sequence $b_j^{(k)} \in \{0,1\}$ of the k^{th} user is a binary bit stream that conveys the information, and ε is a constant. $a_n^{(k)} \in \{-1,+1\}$ is the n^{th} chirp of the k^{th} user, and each frame of T_r seconds contains N_r chirps with duration of T_c seconds per chirp $(T_r = N_r T_c)$.

For PPM-TH-UWB, let $C_j^{(1)}$ in (5) be an independent integer-value and be uniformly distributed over $[0, N_p]$, and let $d^{(k)}_{\lfloor j/N_s \rfloor}$ be independent identically distributed binary data symbols with energy ε_s spreading over N_s frames, the power spectral density (PSD) for $S_1^{(1)}(t)$ can be approximated as [17]

$$\Phi_{uu1}(f) \approx \frac{\varepsilon_s}{T_s} |P(f)|^2 \quad (9)$$

where $P(f)$ is Fourier transform (FT) of $p(t)$. A similar result is also derived in [18] for PAM-TH-UWB.

For PAM-DS-UWB, let the chip sequence satisfy the mean $\mu = 0$ and variance $\sigma^2 = 1$ in (8), and $b_j^{(k)}$ be independent identically distributed binary data symbols, the PSD for $S_4^{(1)}(t)$ can be approximated as [19]

$$\Phi_{uu4}(f) \approx \frac{\varepsilon_s}{T_c} |P(f)|^2 \quad (10)$$

A similar result is also derived in [20] for PPM-DS-UWB. Based on the above-mentioned, the PSD for UWB signal can be given by

$$\Phi_{uu}(f) \approx K_i |P(f)|^2 \quad i = 1,2 \quad (11)$$

where K_i is a constant, K_1 is defined by the symbol energy and the frame duration for TH-UWB, and K_2 is governed by the symbol energy and the chirp duration for DS-UWB.

In order to ensure that $Mask_{jm}(f)$ is a constant, we need to seek a tighter mask $Mask_{jT}(f) \le Mask_j(f)$. A typical task required by the pulse shaper for UWB is to meet the UWB mask, so we let $\Phi_{uu}(f) \le Mask_{jT}(f) \le Mask_j(f)$ for all f . By this, we can get a condition as

$$P(f) \le \sqrt{Mask_{jT}(f)/K_i} \quad i = 1,2 \quad (12)$$

After that, we can obtain $Mask_{jm}$ as follows

$$Mask_{jm} = \begin{cases} \sqrt{Mask_{jTm}(f)/K_i} & f \in B_m \\ 0 & f \notin B_m \end{cases} \quad i = 1,2 \quad (13)$$

We give an example adopting the US FCC mask [1] for seeking the tighter mask $Mask_{jT}(f)$ and dividing sub-bands. As is shown in Figure 4, $B_1 \sim B_8$ are eight continuous sub-bands. The tighter mask $Mask_{jT}(f)$ is given by

$$Mask_{jT}(f) = \begin{cases} -75.3dBm/Mhz, f \in [0, 1.61]GHz \\ -63.3dBm/Mhz, f \in [1.61, 3.1]GHz \\ -41.3dBm/Mhz, f \in [3.1, 10.6]GHz \\ -61.3dBm/Mhz, f \in [10.6, 12]GHz \end{cases} \quad (14)$$

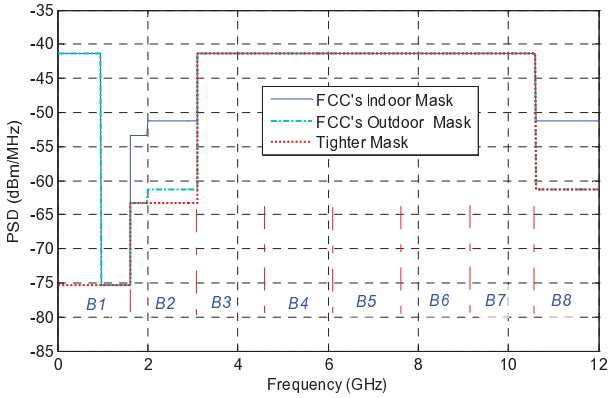

Figure 4 A tighter Mask and a division of the frequency band.

3.1.3. The device implementation

For TDCS, the most effective method for the real-time radio spectrum evaluation is autoregressive (AR) method [21]. The AR method can be implemented by the real-time Fourier transform, and meanwhile, the time domain BF can be generated by the real-time inverse Fourier transform. The real-time transform domain processing technology can be accomplished by SAW devices [22], and the real-time Fourier transform and inverse Fourier transform can be generated based on the multiplication and convolution of desired signal by the linear chirp waveforms through SAW [23]. Furthermore, the M-TDCS can also be performed by SAW devices, so the $S_{UWB-CR1}(t)$ can be implementable by using SAW and some other accessorial devices as well.

3.2. The second proposed pulse

The index for the frequency spectrum of $S_{UWB-CR1}(t)$ matching the UWB mask depends on $Mask_{jm}$, however,

$Mask_{jm}$ is generated based on the tighter mask $Mask_{jT}(f)$, so this index is suboptimal, e.g. in this example adopting FCC UWB mask in Figure 4, this matching index is only 88%. At the same time, because the UWB mask is dissimilar in different countries or regions, $Mask_{jT}(f)$ is also different for the dissimilar UWB mask so as to cause the $Mask_{jm}$ variation in the same sub-band. In order to increase this matching index, and eliminate the weakness of the mask value, and meanwhile, considering the device implementation and the performance of compressed chirp waveform superior to that of the chirp waveform, another novel UWB-CR pulse is proposed by using multiple M-TDCS and a set of compressed chirp waveforms.

3.2.1. Pulse design

Firstly, we still divide the UWB frequency band into M continuous sub-bands $B_m(m = 1, 2, ...M)$, and let the factor C equal one for each M-TDCS. Secondly, let each sub-band B_m employ one M-TDCS to generate one sub-BF $b''_m(n)$, and sum M sub-BFs to get a new time domain BF $b''(n)$. Because $b''(n)$ represents the interference free spectrum for the radio environment, and can change with the electromagnetic environment in real time, we regard $b''(n)$ as an adaptive notch filter. For different UWB masks, we still use a "UWB Spectrum Masks" module to provide different UWB mask–$Mask_j(f)$. The last work is to acquire a signal satisfied the UWB mask $Mask_j(f)$ by using the optimal combination of compressed chirp waveforms, and to let this signal pass this adaptive notch filter to obtain the second new pulse for UWB-CR. A block diagram for this pulse design is illustrated in Figure 5.

Based on the above-mentioned work, $b''(n)$ can be expressed as

$$\begin{aligned} b''(n) &= \sum_{m=1}^{M} b''_m(n) \qquad n = 1, 2, ..., N \\ &= \sum_{m=1}^{M} \frac{1}{N} \sum_{k=1}^{N} A'_m e^{-j(2\pi(k-1)(n-1)/N)} \end{aligned} \tag{15}$$

where N is the point number of inverse Fourier transform, A'_m denotes the vector representing the interference free spectrum of the m^{th} sub-band. The following work is to generate the signal satisfying the UWB mask by using compressed chirp waveforms.

3.2.2. Generating the signal satisfying the UWB mask by using compressed chirp waveforms

Based on (3) and $B_s = |\mu| * T_m$, we know that $p_c(t)$ depends on f_0 , T_m , μ . Because the value for $Mask_j(f)$ is different in each frequency band, we divide $Mask_j(f)$ into I continuous sub-bands W_i based on the different value of $Mask_{ji}(f)(i = 1, 2, ...I)$, and employ one compressed chirp waveform for each sub-band. The i^{th} compressed chirp waveform can be given by

$$f_{i0} = (f_{iL} + f_{iH})/2 \tag{16}$$

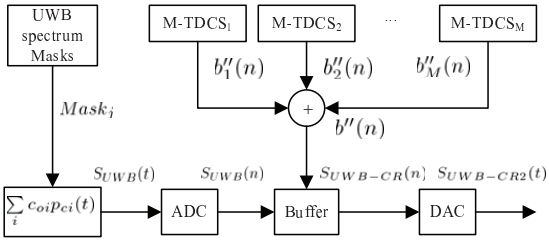

Figure 5 A pluse design for UWB-CR using compressed chirp waveforms and multiple M-TDCS.

$$\mu_i = B_{is}/T_{im} = (f_{iH} - f_{iL})/T_{im} \tag{17}$$

$$PSD(P_{ci}(t)) \le Mask_{ji} \tag{18}$$

In (16),(17),(18), f_{i0} , f_{iL} and f_{iH} denote the center frequency and upper limit frequency and lower limit frequency respectively for the i^{th} sub-band; μ_i , B_{is}, T_{im} are the chirp rate, the frequency-sweep range and chirp duration respectively for the i^{th} compressed chirp waveform $p_{ci}(t)$; $PSD(p_{ci}(t))$, $Mask_{ji}$ are the PSD of $p_{ci}(t)$, the mask vale respectively for the i^{th} sub-band.

We still give an example adopting the US FCC mask for fixing f_{iL}, f_{iH} ,$Mask_{ji}$ and dividing i sub-bands, which is shown in Figure 6.

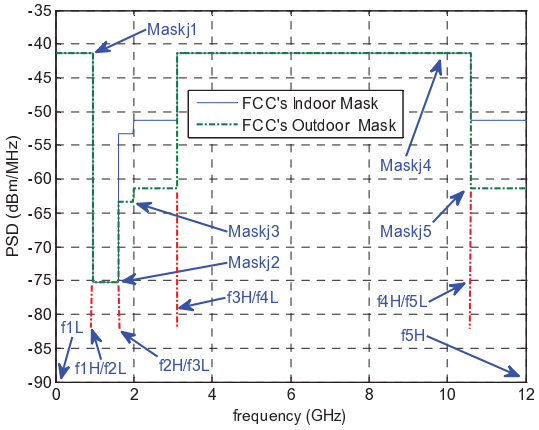

Figure 6 f_{iL}, f_{iH} ,$Mask_{ji}$ for the i^{th} compressed chirp waveforms .

The $Mask_{ji}$ is given by

$$Mask_{ji} = \begin{cases} -41.3dBm/Mhz, f \in [0, 0.96]GHz \\ -75.3dBm/Mhz, f \in [0.96, 1.61]GHz \\ -63.3dBm/Mhz, f \in [1.61, 3.1]GHz \\ -41.3dBm/Mhz, f \in [3.1, 10.6]GHz \\ -61.3dBm/Mhz, f \in [10.6, 12]GHz \end{cases} \tag{19}$$

Since the mask values are different between the frequency band 1.61-1.99GHz and the frequency band 1.99-3.1GHz in Figure 6, and the bandwidth of [1.61,1.99]GHz is very narrow, so we unite these two frequency bands into one band with the mask value -63.3dBm/Mhz in order to reduce the amount of compressed chirp waveform.

By a combination of a few compressed chirp waveforms, we generate the signal $S_{UWB}(t)$, which uses the full frequency band of this mask and meets the requirement of this mask. $S_{UWB}(t)$ can be expressed as

$$S_{UWB}(t) = \overrightarrow{C_o}^T \overrightarrow{P_c} = \sum_i c_{oi} P_{ci}(t) \tag{20}$$

$$\{P_{ci}(t)|f_L{=}f_{iL}, f_H{=}f_{iH}, T_m = T_{mi}, Mask_j = Mask_{ji}\} \tag{21}$$

In (20),(21), $p_{ci}(t), c_{oi}$ denote the i^{th} compressed chirp waveform, and the coefficient of the i^{th} compressed chirp waveform, respectively.

In order to obtain the best matching index with the UWB mask, we utilize the iterative algorithm to get the optimum $\overrightarrow{C_o}$. The procedure is described as follows:

Step 1: Selection. We choose a group of compressed chirp waveforms.

Step 2: Initialization. Using a random way to generate an initial value of $\overrightarrow{C}_o$ named as $\overrightarrow{C}_{os}$. After that, checking whether the PSD of obtained with $\overrightarrow{C}_{os}$ meets the selected mask $Mask_j$.

Step 3: Pre-processing. If $Mask_j$ in the *Step 2* is met, let $\overrightarrow{C}_o = \overrightarrow{C}_{os}$, then skip to *Step 4*, otherwise, repeat *Step 2* until $Mask_j$ is met.

Step 4: Iteration. Since in *step 3* we choose a set of $\overrightarrow{C}_o$, which is not necessarily an optimal PSD for $\overrightarrow{p}_c$. we use an iterative algorithm by changing $\overrightarrow{C}_o$ in (22) so that the PSD of $S_{UWB}(t)$ can approach $Mask_j$ with a best weight coefficient $\overrightarrow{C}_o$.

$$\overrightarrow{C}_o = \begin{cases} \overrightarrow{C'}_o, PSD(\overrightarrow{C}_{os}{}^T \overrightarrow{P}_c) \le PSD(\overrightarrow{C'}_o{}^T \overrightarrow{P}_c) \\ \qquad \le Mask_j \overrightarrow{C}_{os}, \\ Others \end{cases} \tag{22}$$

where $PSD(...)$ denotes the PSD of $S_{UWB}(t)$, the stop condition of the iteration is given by

$0.95 Mask_j \le PSD(\overrightarrow{C}_o{}^T \overrightarrow{P}_c) \le Mask_j$

The signal $S_{UWB}(n)$ can be gained after the $S_{UWB}(t)$ is converted by ADC device.

3.2.3. The proposed pulse

The signal $S_{UWB-CR}(n)$ can be calculated by

$$\begin{aligned} S_{UWB-CR}(n) &= S_{UWB}(n) \otimes b''(n) \\ &= \sum_i c_{oi} p_{ci}(n) \otimes \sum_{m=1}^{M} \tfrac{1}{N} \sum_{k=1}^{N} A'_m e^{-j(2\pi(k-1)(n-1)/N)} \\ &= \sum_l \sum_i c_{oi} p_{ci}(n) \sum_{m=1}^{M} \tfrac{1}{N} \sum_{k=1}^{N} A'_m e^{-j(2\pi(k-1)(n-1-l)/N)} \end{aligned} \tag{23}$$

After the signal $S_{UWB-CR}(n)$ is converted by DAC device, we obtain a novel pulse $S_{UWB-CR2}(t)$ for UWB-CR.

The compressed chirp waveform can also be generated by SAW device [11, 12], so the pulse $S_{UWB-CR2}(t)$ can also be implemented by SAW devices and some other accessorial devices as well.

4. System performance simulation

In this section, we firstly produce these two proposed pulse waveforms, and then evaluate the bit error radio (BER) performance of UWB-CR by using two new pulses. Lastly, we make a comparison between the BER of UWB-CR system by adopting two new puplse and that of UWB system by using the Gaussian pulse.

4.1. Waveform evaluation

Assuming the radio environment to exist two narrowband single-tone jammers, we express these interferences as

$$r_k(t) = A_k \cos(2\pi f_k t) \tag{24}$$

whereA_k , f_k are the amplitude and central frequency for the k^{th} interference, respectively.

We assume $f_1 = 3.5GHz$ for worldwide interoperability for microwave access (WiMax), and $f_2 = 5.3GHz$ for wireless local area networks (WLAN).

4.1.1. The first proposed pulse waveform

The multiple M-TDCS sense the radio environment, and generate $S_{UWB-CR1}(t)$. The UWB mask adopts FCC's mask (see Figure 4), and the parameters in simulation are listed in Firgure 7. $S_{UWB-CR1}(t)$ and its spectrum are illustrated in Figure 8, in which the top plot shows the spectrum of $S_{UWB-CR1}(t)$, and the bottom plot shows $S_{UWB-CR1}(t)$. From Figure 8, we know that the spectrum efficiency for $S_{UWB-CR1}(t)$ is approximatively one, and the index for the spectrum of $S_{UWB-CR1}(t)$ matching the UWB mask can be given by (12-0.96-(1.99-1.61)-0.2)/12=87.2%.

4.1.2. The second proposed pulse waveform

The multiple M-TDCS sense the radio environment to generate $b''(n)$, and the UWB mask adopts FCC's mask, and the sub-bands dividing is shown in Figure 7. The $b''(n)$ and its spectrum are illustrated in Figure 9, in which the top plot shows the spectrum of $b''(n)$, and $b''(n)$ is shown in the bottom plot.

For the pulse $S_{UWB}(t)$, we still adopt the FCC's spectrum mask, and the parameters f_{iL} , f_{iH} ,$Mask_{ji}$ are shown in Figure 6. The pulse and its spectrum are illustrated in

B_m (GHz)							
B_1	B_2	B_3	B_4	B_5	B_6	B_7	B_8
0~ 1.61	1.61~ 3.1	3.1~ 4.6	4.6~ 6.1	6.1~ 7.6	7.6~ 9.1	9.1~ 10.6	10.6~ 12

$Mask_{jTm}(f)$							
B_1	B_2	B_3	B_4	B_5	B_6	B_7	B_8
2.95×10^{-11}	4.67×10^{-10}	7.4×10^{-8}					7.4×10^{-10}
PPM-TH-UWB		K_1=2.4					
PAM-DS-UWB		K_2=3.2					

Figure 7 The parameters in simulation.

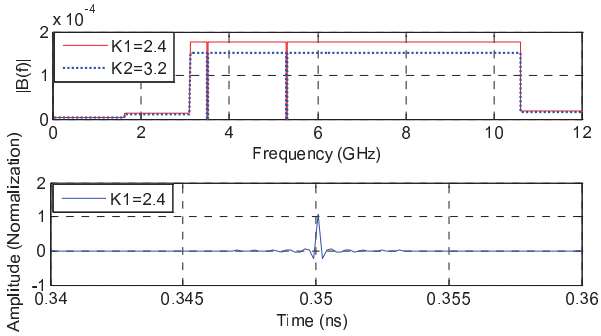

Figure 8 The first new pulse for UWB-CR and its spectrum.

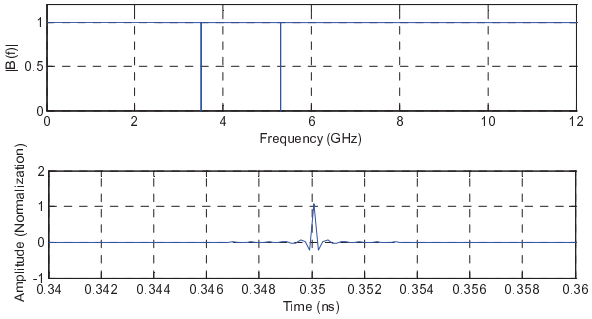

Figure 9 The new BF $b''(n)$ and its spectrum.

Figure 10, in which the top plot shows $S_{UWB}(t)$, and the spectrum of $S_{UWB}(t)$ is shown in the bottom plot.

Based on $b''(n)$ and $S_{UWB}(n)$, Figure 11 shows the pulse $S_{UWB-CR2}(t)$.

From Figure 9 and Figure 10, we know that the spectrum efficiency for $S_{UWB-CR2}(t)$ is also approximatively one. Based on the generated procedure of $S_{UWB}(t)$, the index for the frequency spectrum of $S_{UWB}(t)$ matching the UWB mask is no less than 95%, so the matching index $S_{UWB-CR2}(t)$ can be given by 0.95-(0.2/12)= 93.3%.

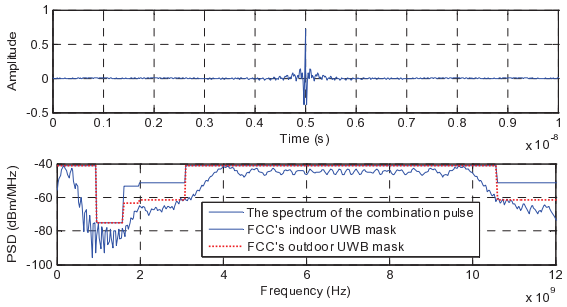

Figure 10 The combinated signal of compressed chirp waveforms and its spectrum .

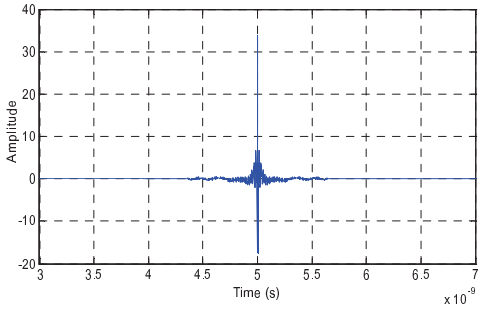

Figure 11 The new pulse $S_{UWB-CR2}(t)$ for UWB-CR .

4.2. BER performance evaluation

4.2.1. The first proposed pulse

We evaluate the BER performance by using two new pulses in such two typical modulations of IR-UWB as PPM-TH-UWB and PAM-DS-UWB. The utilizes the full interference free spectrum of FCC's UWB mask, however, in order to satisfy the FCC's UWB mask and maintain the pulse bandwidth as wide as possible in UWB system, at least the seventh order or higher derivative of the Gaussian pulse should be used [24], so we compare the BER performance of $S_{UWB-CR1}(t)$ with UWB system by using the seventh order derivative of Gaussian pulse through the computer simulation. The time width and shape factor of the seventh order Gaussian pulse are 10ns and 0.2ns, respectively. For (5) and (8),$k = 1$, $C_j \in \{1, 2, 3\}$,$N_p = 3000$

,$T_d = 0.5ns$,$T_c = 1ns$, $\varepsilon = 0.25$, $T_s = T_r = 9ns$, $N_s = N_r = 3$. The average transmitted powers of UWB systems are all -41.3dBm in the simulation.

With the assumption that the radio environment is an additive white Gaussian noise (AWGN) with two narrowband single-tone jammers, the BER values of systems are shown in Figure 12. In Figure 12, CR-PPM-TH-UWB and CR-PAM-DS-UWB are the BER performance of UWB-CR systems by using the pulse $S_{UWB-CR1}(t)$; Gaussian-PPM-TH-UWB and Gaussian-PAM-DS-UWB are the BER performance of UWB systems by using the seventh order derivative of Gaussian pulse. From Figure 12, we can conclude the BER performance of UWB-CR systems can be improved about 2-3dB compared with that of UWB systems.

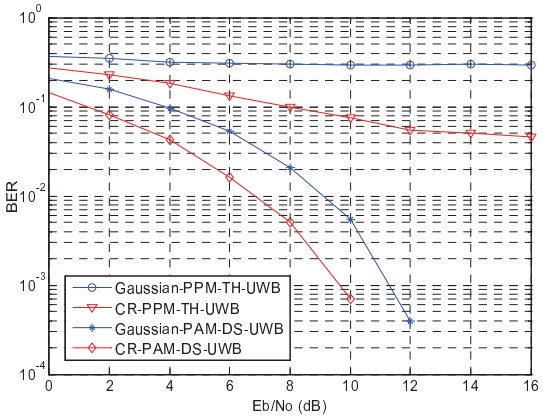

Figure 12 BER versus E_b/N_0.

4.2.2. The second proposed pulse

In order to get BER performance evaluation of the second proposed pulse, we still evaluate the BER performance by using the pulse $S_{UWB-CR2}(t)$ in PPM-TH-UWB and PAM-DS-UWB, and compare the BER performance of the second proposed pulse with the seventh order derivative of Gaussian pulse through the computer simulation. The time width and shape factor of the seventh order Gaussian pulse are 10ns and 0.2ns, respectively. For (5) and (8), $k = 1$, $C_j \in \{1, 2, 3\}$,$N_p = 3000$,$T_d = 0.5ns$,$T_c = 1ns$, $\varepsilon = 0.25$, $T_s = T_r = 30ns$, $N_s = N_r = 3$.The average transmitted powers of systems are all -41.3dBm in the simulation. The radio environment is the same as that of the first proposed pulse. The BER values of systems are shown in Figure 13.

In Figure 13, CR-PPM-TH-UWB and CR-PAM-DS-UWB are the BER performance of UWB systems by using the pulse $S_{UWB-CR2}(t)$; Gaussian-PPM-TH-UWB and Gaussian-PAM-DS-UWB are the BER performance for the seventh order derivative of the Gaussian pulse.From Figure 13, we also can conclude that the second new pulse also improves the BER performance for UWB systems.

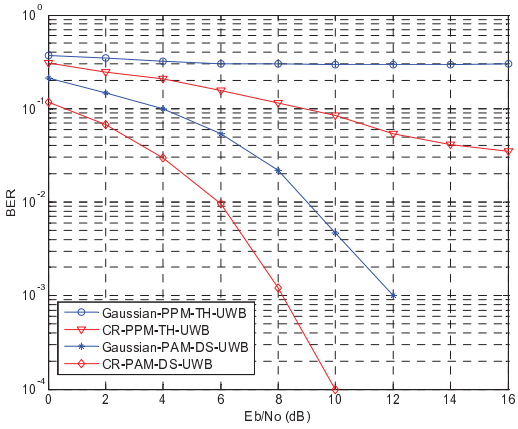

Figure 13 BER versus E_b/N_0 .

5. Conclusion

Using multiple M-TDCS, this paper proposes two novel pulse generation methods that are capable of sensing the communication scene in each sub-band, and comply with the UWB power spectral mask. The two new pulses can be implemented by using SAW and some other accessorial devices as well, and may utilize the full frequency band for the UWB mask, and greatly improve the utilizing efficiency of UWB spectrum. Because it is difficult for the Gaussian seventh order derivative to be implemented, so the anti-jamming capability and realizability of two new pulses are more excellent than that of the Gaussian seventh order derivative pulse. Since both new pulses utilize multiple M-TDCS to sense the radio environment, the complexity for UWB-CR system adopting two pulses will be added and how to avoid it is worth further research.

Acknowledgement

This work was supported by PetroChina Innovation Foundation (No. 2010D-5006-0703), and the Research Fund for Higher Education of Inner Mongolia Autonomous Region (No. NJ10012), and the Scientific Research Initial Fund for Higher Talents Program of Inner Mongolia University, China.

References

[1] Federal Communications Commission, U.S., FCC 02-48, ET Docket No. 98-153, 2(2002).

[2] Federal Communications Commission, U.S., FCC 03-322, ET Docket No. 03-108, 2(2003).
[3] H. G. Zhang, X. F. Zhou, K. Y. Yazdandoost and I. Chlamtac, IEEE Journal on Selected Areas in Communications **24**, 878(2006).
[4] S. Haykin, IEEE Journal on Selected Areas in Communications **23**, 216(2005).
[5] V. D. Chakravarthy, A. K. Shaw, M. A. Temple and J. P. Stephens, Proc. 2005 IEEE Wireless Communications and Networking Conference **2**, 724(2005).
[6] V. Chakravarthy, A. S. Nunez and J. P. Stephensl, IEEE Communications Magazine **43**, S11(2005).
[7] A. Mehbodniya and S. Aissa, Proc. 2007 IEEE Global Telecommunications Conference, 5200(2007).
[8] R. Fisher, R. Kohno, H. Ogawa, H. g. Zhang, K. Takizawa, M. M. laughlin and M. Welborn. IEEE P802.15-04/0137r4, 5(2005).
[9] Y. Wang, X. D. Dong and I. J. Fair, IEEE Transactions on Wireless Communications **6**, 1944(2007).
[10] The Office of Communications, U.K., Decision to make the wireless telegraphy (ultra-wideband equipment) (exemption) regulations 2007, (2007).
[11] D. P. Morgan, Surface-Wave Devices for Signal Processing, 2nd ed. (Elsevier, Amsterdam, 1991).
[12] A. Springer, W. Gugler, M. Huemer, R. Koller and R. Weigel, IEEE Transactions on Microwave Theory Techniques **49**, 754(2001).
[13] H. B. Shen, W. H. Zhang and K. Y. Kwak, ETRI Journal **29**, 676(2007).
[14] H. P. Liu, IEEE Journal on Selected Areas in Communications **24**, 885(2006).
[15] M. Z. Win and R. A. Scholtz, IEEE Transactions on Communications **48**, 679(2000).
[16] W. Cao, A. Nallanathan and C. C. Chai, Proc. 2006 IEEE Global Telecommunications Conference, 1(2006).
[17] X. Luo, L. Yang and G. B. Giannakis, Journal of Communications and Networks **5**, 344(2003).
[18] X. R. Wu, Z. Tian, T. N. Davidson and G. B. Giannakis, IEEE Transactions on Signal Processing **54**, 2009(2006).
[19] Z. Ye, A. S. Madhukumar and F. Chin, Proc. 2004 IEEE International Conference on Communications **6**, 3561(2004).
[20] M. G. D. Benedetto and G. Giancola, Understanding ultra wide-band radio fundamentals, 124(Prentice Hall Professional Technical Reference Pearson Education, Inc., New Jersey, 2004).
[21] M. L. Roberts, M. A. Temple, R. A. Raines and E. P. Magee, Proc. 21st Century Military Communications Conference Proceedings **2**, 1119(2000).
[22] L. B. Milstein and P. K. Das, IEEE Transactions on Communications **25**, 841(1977).
[23] L. Milstein and P. Das, IEEE Transactions on Communications **28**, 816(1980).
[24] H. S. Sheng, P. Orlik , A. M. Haimovitch, L. J. Jr. Cimini and J. Y. Zhang. Proc. 2003 IEEE International Conference on Communications **1**, 738(2003).

Shubin Wang is with College of Electronic Information Engineering, Inner Mongolia University,China. He received his BS and MS degree from the Inner Mongolia University,China in 1996 and 2003,respectively; and the PhD degree from the Beijing University of Posts and Telecommunications in 2010. In 2009-2010, he was a Research Fellow supervised by Prof. Kyung Sup Kwak in Inha University, Inchon, Korea. His current research interests involve wideband wireless communication technology, UWB wireless communications, and cognitive radio, and he published over 20 papers.

Zheng Zhou is with School of Information and Communication Engineering, Beijing University of Posts and Telecommunications(BUPT). He received his Master and Doctor degree of Electrical Engineering in BUPT in 1982 and 1988, respectively. In 1993-1995, he was a Visiting Research Fellow in Chinese University of Hong Kong, supported by the Hong Kong Telecom International Postdoctoral Fellowship. In 2000, he visited Japan Kyocera DDI Research Institute as an Invited Overseas Researcher supported by Japan Key Technology Center. His current research interests involve short-range wireless technology, UWB wireless communications, and cognitive radio, and he published over 300 papers. He is the committee member of TCCN IEEE ComSoc.

Kyung Sup Kwak is a member of IEEE, IEICE, KICS, and KIEE. He received the BS degree from Inha University, Inchon, Korea, in 1977; the MS degree from the University of Southern California in 1981; and the PhD degree from the University of California at San Diego in 1988, under the Inha University Fellowship and the Korea Electric Association Abroad Scholarship Grants. From 1988 to 1989, he was a member of technical staff at Hughes Network Systems, San Diego, California. From 1989 to 1990 he was with the IBM Network Analysis Center at Research Triangle Park, North Carolina. Since then, he has been with the School of Information and Communication, Inha University, Korea, as a professor. He was the chairman of the School of Electrical and Computer Engi-

neering from 1999 to 2000 and the dean of the Graduate School of Information Technology and Telecommunications from 2001 to 2002 at the Inha University, Inchon, Korea. He is currently with the UWB Wireless Communications Research Center, a key government IT research center in Korea. He is now Inha Fellow Professor (IFP). Since 1994, he has been a member of the Board of Directors, and was the vice president of the Korean Institute of Communication Sciences (KICS) from 2000 to 2002. He was the president of KICS in 2006. His research interests include multiple access communication systems, mobile communication systems, UWB radio systems and ad-hoc networks, as well as high-performance wireless Internet.